

ACTA ADRIATICA
INSTITUT ZA OCEANOGRFIJU I RIBARSTVO — SPLIT
SFR JUGOSLAVIJA

Vol. XVIII, No. 13

**GEOSTROPHIC CURRENTS IN THE SOUTHEASTERN
SECTOR OF THE MEDITERRANEAN SEA**

GEOSTROFIČKE STRUJE U JUGOISTOČNOM DIJELU MEDITERANA

SAYED H. SHARAF EL DIN AND AMIN KARAM

SPLIT 1976

GEOSTROPHIC CURRENTS IN THE SOUTHEASTERN SECTOR OF THE MEDITERRANEAN SEA

GEOSTROFIČKE STRUJE U JUGOISTOČNOM DIJELU MEDITERANA

Sayed H. Sharaf El Din

Department of Oceanography, Alexandria University, Alexandria, Egypt

and

Amin M. Karam

Institute of Oceanography and Fisheries, Alexandria, Egypt

INTRODUCTION

Direct current measurements over the continental shelf off the Nile Delta are very scarce. Only five measurements have been taken from a few localities by international research vessels and by the Suez Canal Authority (Sharaf El Din, 1972).

The common feature of the current system along of the Egyptian coast is a west to east flow. Before the construction of the Aswan Dam, the effect of the Nile flood along the coast was noticeable to a few km away from the coast and to maximum depth of 100 m (Sharaf El Din, 1972; Gorgy, 1966). During the winter, the current pattern is different from that in the summer. This difference is attributed primarily to wind action. Different investigators have attempted to formulate the circulation pattern in the Mediterranean Sea (Ovtchinnikov, 1966), while others investigated the current regime in the area between the Lebanese coast and Cyprus (Engel, 1967).

In this paper, the dynamic topography at the different levels will be studied using the temperature, salinity and density observations over the continental shelf in the area bounded by the south and east coasts of the Mediterranean Sea, Lat. 34° N and Long. 27° E. In addition, the water characteristics and the geostrophic current will be clarified.

METHODS AND MATERIALS

The data used in this study were collected by different research vessels including CALYPSO (22 to 23 October 1956), VAVILOV (3 to 6 October 1959, 16 October 1964), SHOYO-MARU (17 to 21 March 1959), OVČICA (16 to 20 October 1960), GOLUBICA (4 to 11 October 1961), CHYPRE 04 (19 to 20 February 1965), ICHTHYOLOG (6 to 14 October 1966, 11 to 14 September 1970).

These observations were taken during the flood period (September-October), before and after the construction of Aswan High Dam and in the winter season (non-flood season). Fortyfive hydrographic stations were taken during September-October before the construction of the High Dam and 49 stations were taken after the stoppage of the Nile flood. During the winter season only fortyone stations were used in these analyses. Figures 1, 2 and 3 show the location of the hydrographic stations used.

According to Defant, the most practical and logical method of choosing the reference level is the one developed by him (Defant, 1941). The reference level was calculated using this method only at the deep stations. In the shallow parts of the investigated area, the method of Groen (1948) was applied where the depths were less than the depth of the reference level computed for the deep stations. In this method the isosteres on each level in the imaginary water mass (solid part) have a constant slope equal to the slope of the isosteres at the point where it meets the bottom line. From the dynamic height computations, geopotential topography charts for the surface, 50 db and 100 db relative to the selected reference level were made. These charts represent the flood period before and after the High Dam as well as the winter season. Geostrophic velocity profiles were made for different pairs of stations and were plotted for the three periods mentioned above.

RESULTS

Water Characteristics

The water masses in the investigated area (Figures 1, 2 and 3) are identified during the flood season before and after the High Dam and during the winter season. Figure 4 shows temperature versus salinity for the observations taken in the area during the flood period before the High Dam. The effect of the Nile flood is indicated in the T-S curve by surface coastal water of low salinity (26 to 36‰) and high temperature (22 to 26°C). The effect of the Nile flood disappeared at the offshore surface stations as shown in Figure 5, resulting in surface water of high salinity (39 to 39.4‰) and high temperature (about 19 to 25°C). A layer of subsurface minimum salinity (less than 39‰) and low temperature is observed between 50 m to 100 m. Below 100 m, the salinity increases slightly while the temperature decreases. The deep water (below 300 m) is characterised by low salinity (38.6 to 39.0‰) and low temperature (13.3 to 14.8°C).

The stratification of the water masses during the same season, after the disappearance of the Nile flood due to the construction of the High Dam,

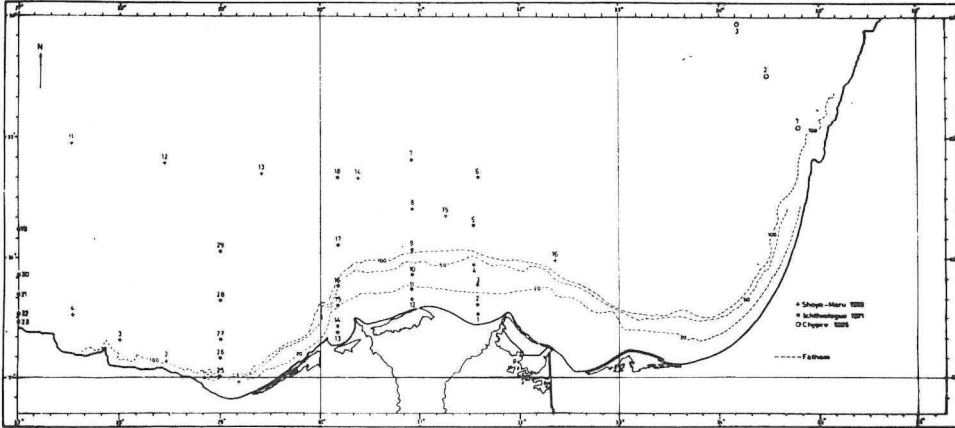


Fig. 3 — Map showing the location of the hydrographic stations taken during the winter season (February–March) of different years.

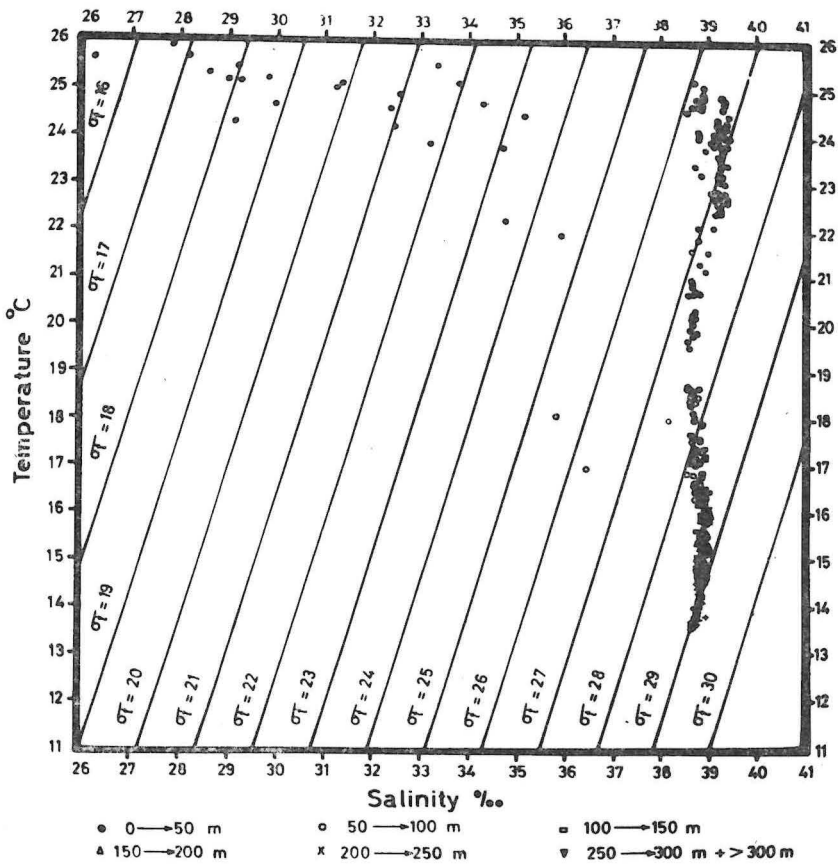


Fig. 4 — Temperature versus salinity for all observations taken in the investigated area during the flood period before the High Dam.

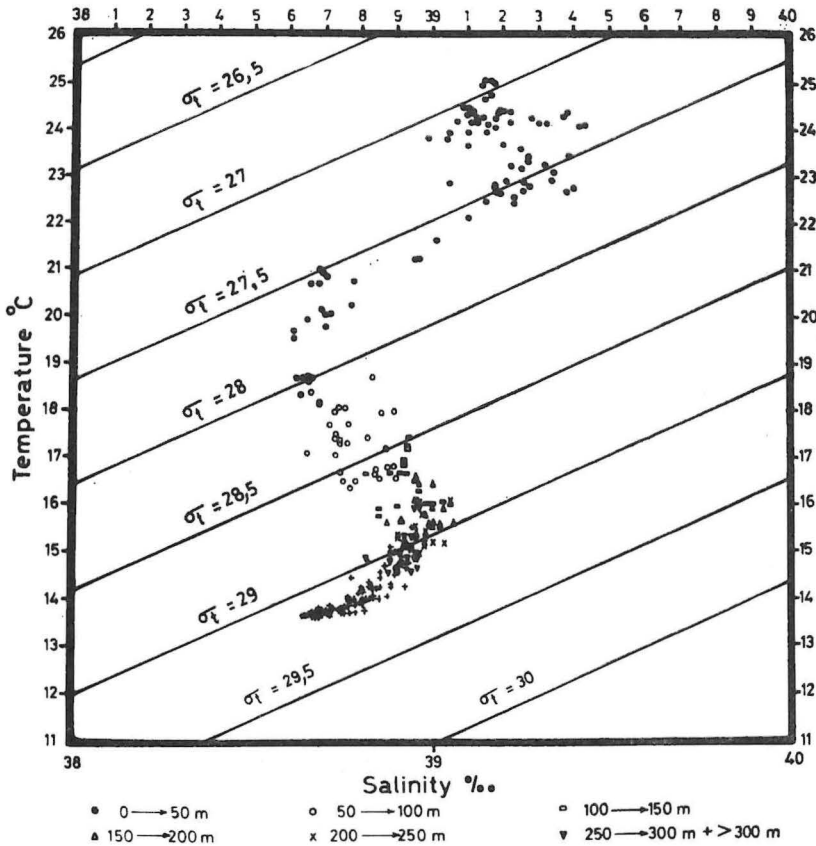


Fig. 5 — Temperature versus salinity for all observations taken in the investigated area between Lat. 32°N to 34°N during the flood period before High Dam.

(σ_t around 28.5). The salinity shows a slight decrease in the subsurface layer (50 to 100 m), followed by a slight increase at the intermediate layer (100 to 300 m). The deep water again shows a slight decrease in salinity. However, the differences in salinity are much less than in summer and indicate a great homogeneity due to the winter convection. The σ_t values reflect such a small stability.

The bottom water remains almost the same during most of the season. The bottom water (below 300 m) has a salinity of about 38.8‰ and temperature 13.5°C (σ_t —29.2), similar to that which was observed during September and October. The bottom water masses correspond exactly to those found by Pollak (1951) and Wüst (1961) in the area.

Geopotential Topography.

During the flood period before the High Dam.

The reference level is a necessary parameter to convert the geopotential anomalies into geopotential topography. In the coastal stations, the level

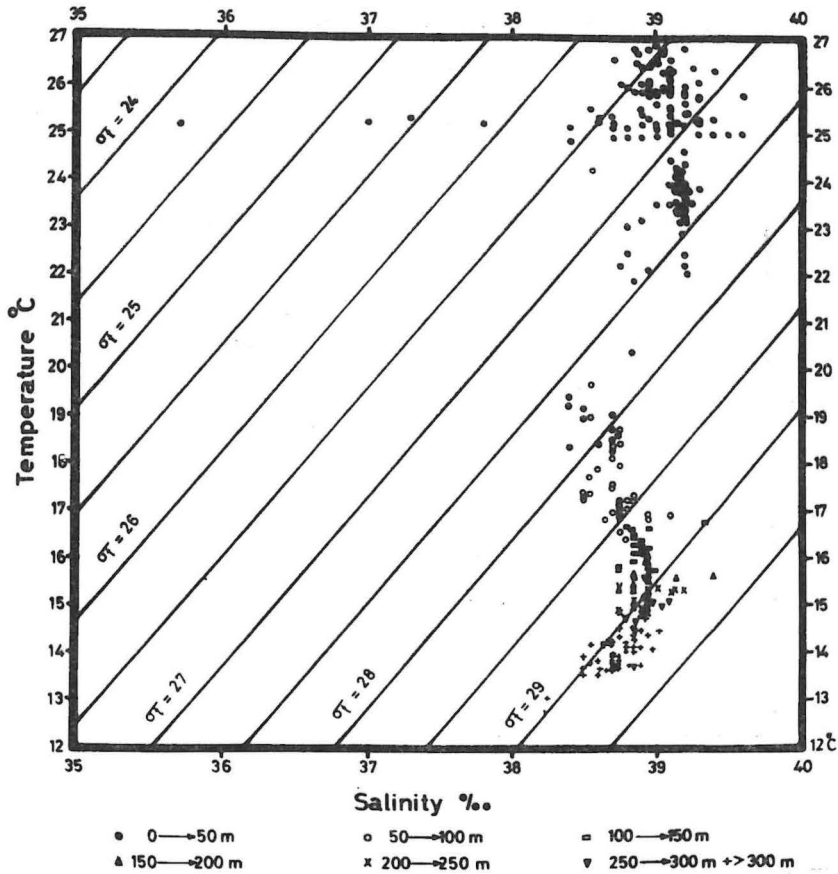


Fig. 6 — Temperature versus salinity for all observations taken in the investigated area during the non-flood season after the High Dam (September–October).

of no motion was calculated using the interpolation method of Groen (1948). At the offshore stations, the level of no motion was found to be between 200 and 300 m below the surface. The data used in the calculation for the period prior to the construction of the Aswan High Dam were taken from different stations during October of different years (Figure 1).

The geopotential topography for the surface, 50 m, and 100 m below the surface relative to the selected reference level of the pair of the stations are plotted in Figure 8.

The geopotential topography and associated circulation pattern near the coast follow the general trend of the flow in the Mediterranean Sea from west to east. At the surface the effect of the Nile flood is indicated by the strong concentration of the isobars in front of the Nile Delta. This flow slightly diminishes in intensity eastwards. The general flow near the eastern

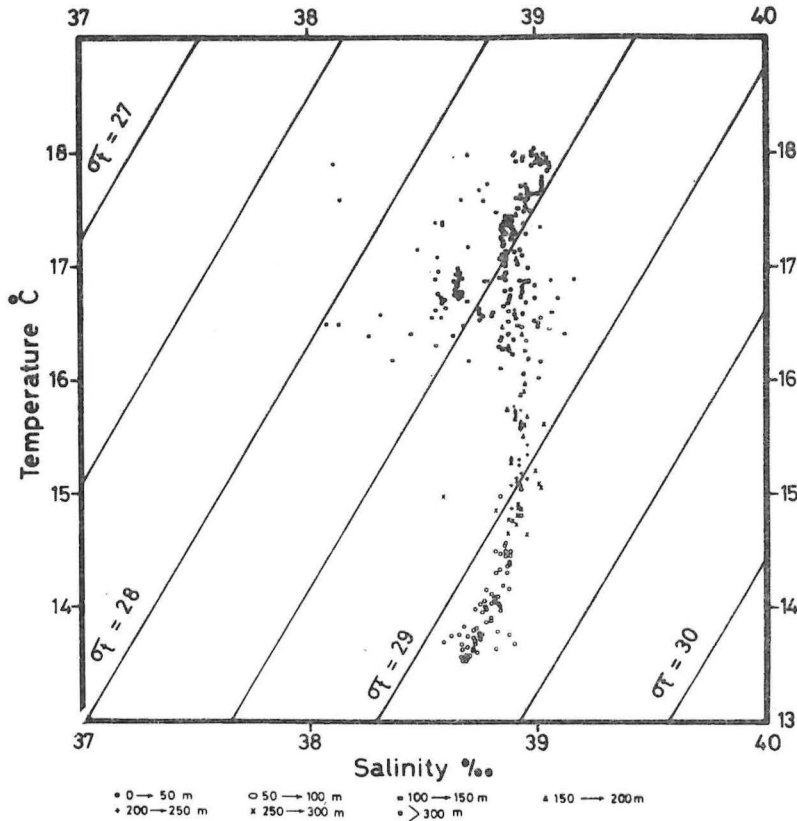


Fig. 7 — Temperature versus salinity for all observations taken in the investigated area during the winter season (February–March).

Mediterranean coasts of Israel and Lebanon is northward. Away from the coast, at a distance of 10 to 20 km, the flow turns southwesterly. The origin of this reverse could not be traced from this study but it may originate somewhere near Cyprus. This trend was predicted from the current measurements taken by the CALYPSO in 1956 (Lacombe and Tchernia, 1960) and was also noted by Emery and George (1963).

The cyclonic eddy found in the surface layer at Lat. 33°N and Long. 28°E disappears at depths 50 m and 100 m. The anticyclonic eddy off the Lebanese coast is strongly developed at the 50 m and 100 m depths. In general, the flow pattern at 50 m and 100 m resembles very closely that at the surface with various eddies at different spots. The data after construction of the Aswan High Dam are insufficient to make a reliable analysis.

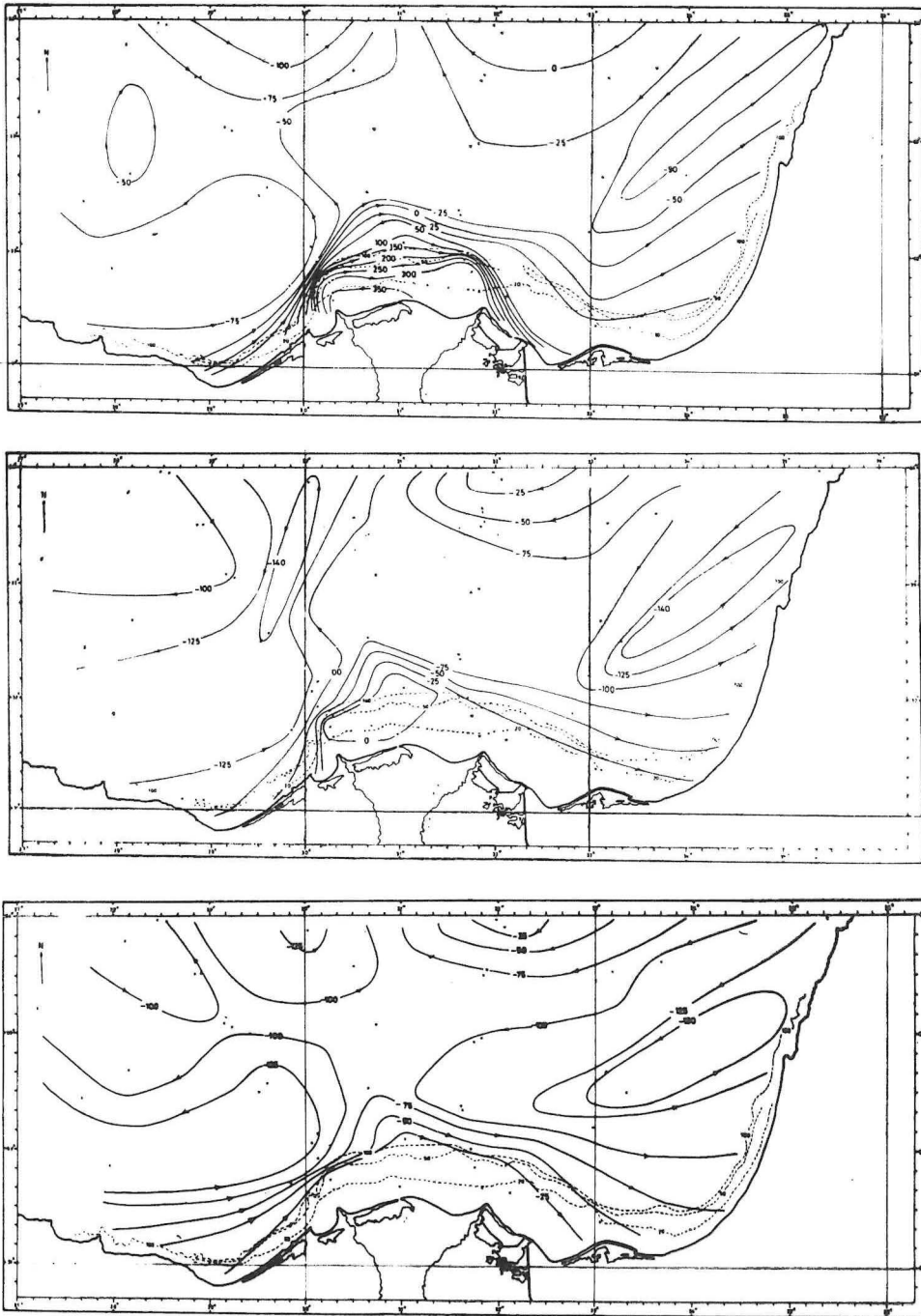


Fig. 8 — Geopotential topography (in dy. mm) relative to the selected reference level during October before the High Dam: a — surface; b — 50 db; c — 100 db.

During the winter season

The hydrographic stations used in these computations are those of February—March of the years 1959, 1965 and 1971 (Figure 3). The dynamic topography of the area under investigation at the surface, 50 m and 100 m below surface is shown in Figure 9. The topography of the sea surface relative to the selected reference level agrees with the general flow pattern in the Mediterranean Sea. The geostrophic flow is almost parallel to the North African coast and then is deflected to a northeasterly direction along the Lebanese coast.

At Lat. 32°N, in front of the Suez Canal, a cyclonic eddy is developed at the surface and is strengthened at depths 50 m and 100 m below surface. Another cyclonic eddy exists at the surface at Lat. 33°N and Long. 28° to 29° E. This cyclonic eddy also persists at other depths (Figure 9). The surface eddy may be attributed to the prevailing northwest wind during winter. At depths of 50 m and 100 m below the surface, the flow pattern resembles very closely that at the surface.

Geostrophic Circulation.

Before the High Dam.

In this section the vertical distribution of the geostrophic flow is investigated during the flood period (September—October). The geostrophic velocity was calculated from the dynamic topography using the standard procedure. During the flood and before the High Dam, the velocity of the water flow near the branches of the Nile reached 300 cm/sec. During the flood period and in summer, the atmospheric condition is fairly stable. In this case the geostrophic circulation constitutes the principal component of the total circulation.

Using the dynamic computations, six stations shown in Figure 1 (39, 40, 41, 42, 44, 45) were taken in the shallow area off the Nile Delta affected by the flood. Six other stations shown in Figure 1 (78, 79, 80, 85 and 86) were taken in the deeper areas away from the effect of the Nile flood. The geostrophic current was calculated between each set of two stations taken in the area under consideration. Each two stations were taken in a direction perpendicular to the coast to obtain the current parallel to it since the main current is from west to east. Figure 10 shows the geostrophic velocity profile at the onshore stations where the effect of the Nile flood flow is clear. The velocity of the flow deduced from the dynamical computations at these stations ranges from about 200 cm/sec at the mouth of the two branches of the Nile to 120 cm/sec in front of Lake Burollos and, as can be expected, is directed to the east at different depths. The calculated geostrophic current agrees with the measurement taken by the R/V *OVČICA* during October 1960 (Gorgy, 1966). The surface velocity measured by the Ekman current meter during October 1960 was 4 to 6 knots (Gorgy, 1966) over the continental shelf in front of the Nile Delta. This velocity drops to a minimum of 6 cm/sec off the Lebanese coast but sometimes reaching a maximum of about 25 cm/sec (Emery and George, 1963). Figure 11 shows the geostrophic velocity

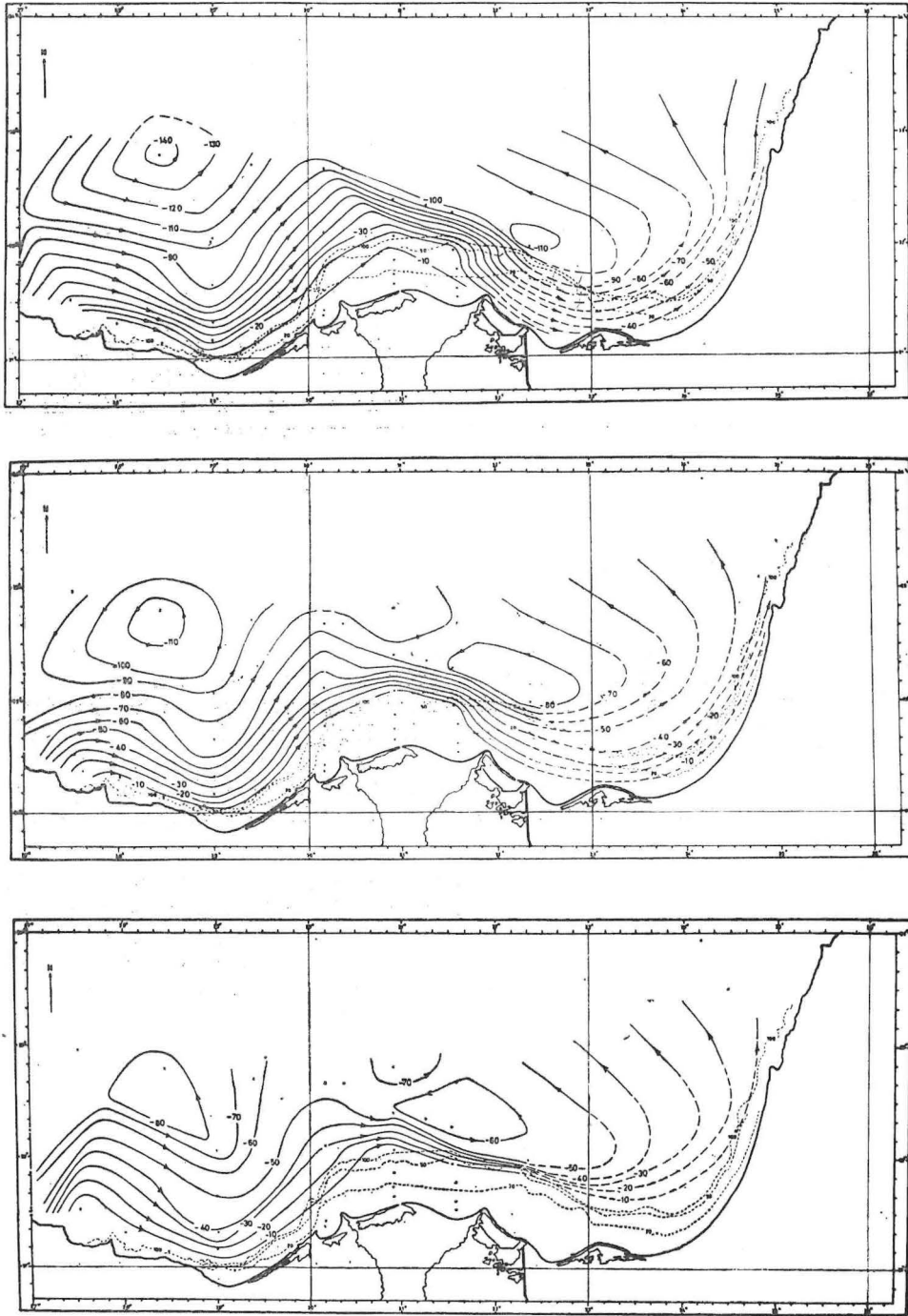


Fig. 9 — Geopotential topography (in dy. mm) relative to the selected reference level during winter (February—March): a — surface; b — 50 db; c — 100 db.

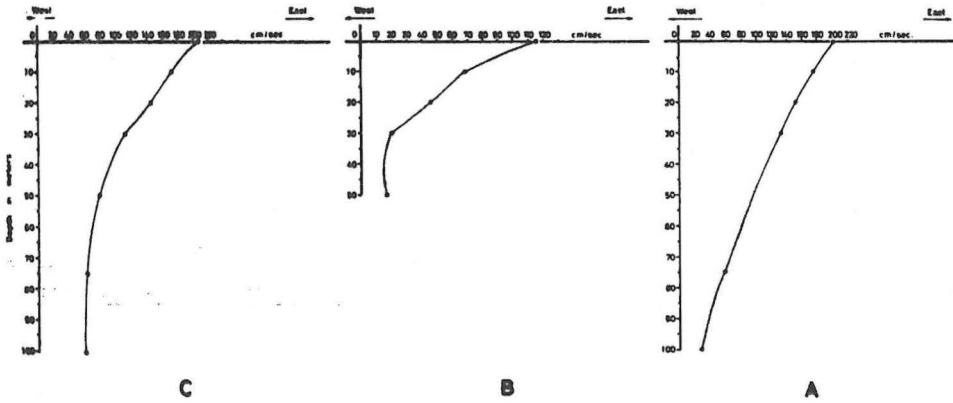


Fig. 10 — Geostrophic velocity profiles between selected pairs of onshore stations during October before the High Dam: a — flow between stations 39 and 40; b — flow between stations 41 and 42; c — flow between stations 44 and 45.

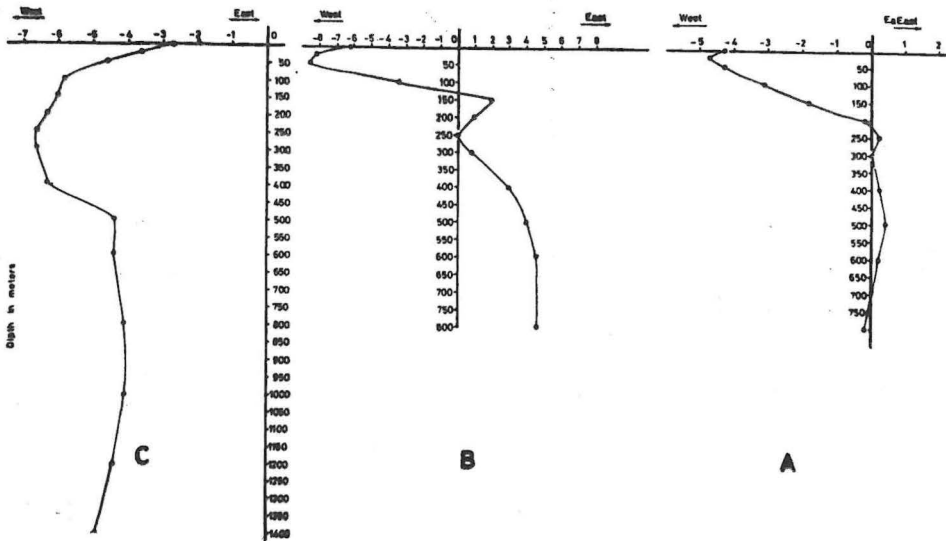


Fig. 11 — Geostrophic velocity profiles between selected pairs of offshore stations during October before the completion of High Dam: a — flow between stations 78 and 79; b — flow between stations 80 and 81; c — flow between stations 85 and 86.

profile between offshore pairs of stations 78 and 79, 80 and 81, and 85 and 86 respectively. At the surface, the flow is directed to the west with maximum velocity of 8 cm/sec. The velocity profile between stations 79 and 78 (Figure 11) gives three levels of zero motion, at 230, 300 and 700 m respectively. In

Figure 11b, the velocity profile shows two levels of no motion at depths 130 m and 250 m below surface with a velocity direction to the east at the bottom layers. Between stations 85 and 86, the geostrophic velocity profile from the surface to bottom is in the west direction at all depths.

After the High Dam, twelve other stations were taken, six inshore (15, 16, 9, 10, 3, 4) and six offshore (13, 14, 11, 12, 5 and 6). Only the profiles of the geostrophic flow of the offshore stations will be discussed in detail. Figure 12 shows the geostrophic velocity profile between the pair of the stations, 14 and 13, 11 and 12, and 5 and 6 respectively. The magnitude of the calculated velocity at different depths is fairly similar to that observed by Guibout (1972) at Lat. $33^{\circ} 52' N$ and Long $30^{\circ} 34' E$ in October 1968.

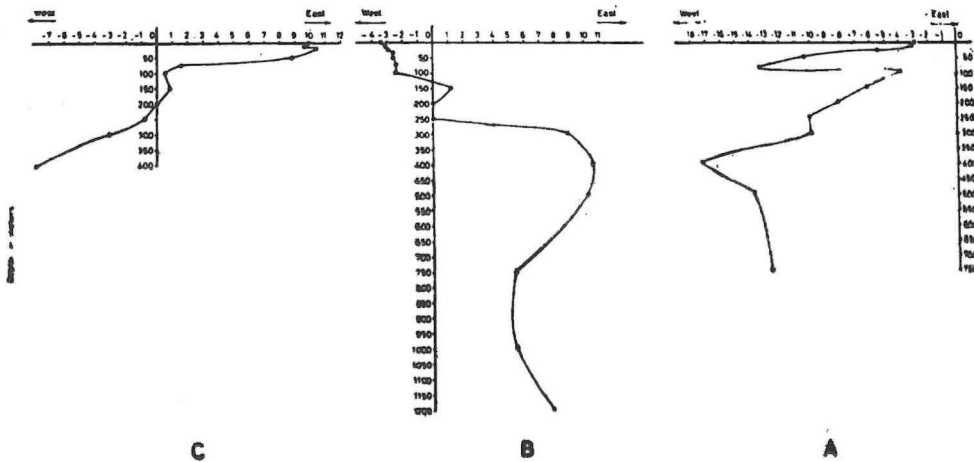


Fig. 12 — Geostrophic velocity profiles between selected pairs of stations during the flood season after High Dam: a—flow between stations 5 and 6; b—flow between stations 11 and 12; c—flow between stations 13 and 14.

The velocity profile between stations 14 and 13 (Figure 12), gives an easterly flow at the surface and to a depth of 200 m and then westerly flow in the rest of the layers. Between stations 11 and 12, the velocity profile (Figure 12) gives a westerly inflow in the surface layer, then easterly inflow below 250 m. A westerly flow is seen between stations 5 and 6 at all depths. The maximum velocity reaches about 18 cm/sec at the surface layer and 12 cm/sec in the deep layers. This indicates the same pattern observed before the High Dam, as expected.

During the winter season

During the winter season, when the intermediate water of high salinity is observed in the Levant basin, the geostrophic velocity profile at the offshore stations is different from one station to another. Between stations 17 and 18 (Figure 13) the velocity profile gives an easterly flow in the surface layer with a maximum velocity of 18 cm/sec and a westerly flow below

200 m. The flow between stations 7 and 8 (Figure 13) is directed to the east at all depths with maximum velocity of 22 cm/sec at 300 m. Again the geostrophic velocity profile between stations 5 and 6 gives an easterly flow down to 250 m westerly flow below that depth. This variation in the velocity profile from one station to another can be attributed to the effect of the cyclonic eddies which exist in the area.

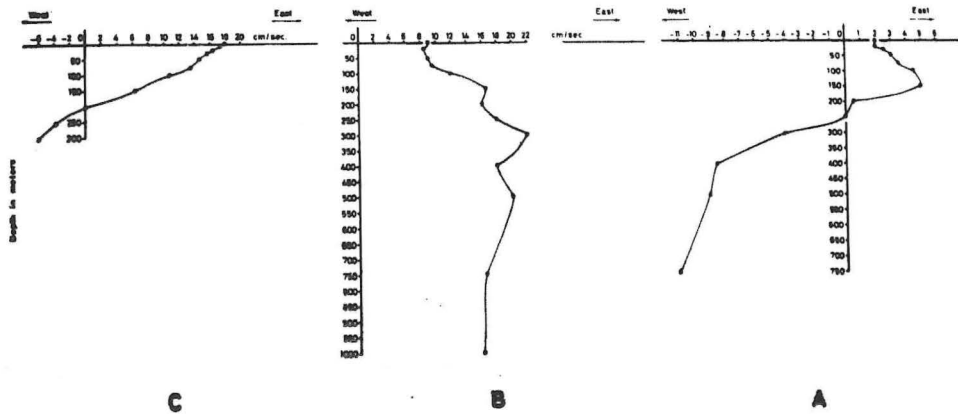


Fig. 13 — Geostrophic velocity profiles between selected pairs of onshore stations during winter season: a—flow between stations 5 and 6; b—flow between stations 7 and 8; c—flow between stations 17 and 18.

DISCUSSION AND CONCLUSIONS

Direct current measurements in the southeastern sector of the Mediterranean Sea are very scarce. For this reason, the current pattern computed from the oceanographic data provides information on the general circulation off the Egyptian Mediterranean coast. The dynamic computation for determining the geostrophic current depends to a great extent on the choice of the reference level. At deep stations there are no problems, while at the shallow stations the uncertainty in the choice makes it difficult to rely upon the result.

The effect of the Nile flood is clearly indicated in the chart of the geopotential topography of the surface. The effect diminishes towards the east and towards the bottom. Also this effect is indicated on the T-S diagrams during the period September—October before and after the erection of the High Dam.

The coincidence of high temperature (22 to 26°C) and low salinity (26 to 36‰) shown in the T-S diagram clearly characterizes the effect of the Nile flood. This body of water disappeared after damming of the Nile. The water circulation off the eastern coast of Mediterranean Sea turns to a south-westerly direction as observed by Lacombe and Tchernia (1960) and Emery and George (1963).

The geopotential topography at different depths referred to the selected reference level represent the condition clearly at that depth during the period of investigation. A good indication of that representation is the agreement between the calculated and observed velocities at some locations in the investigated area. The water masses in the southeastern sector of the Mediterranean Sea vary from one season to another. In winter, the Levant water of high salinity and high temperature exists in the layer 100 to 300 m. The surface waters, on the other hand, are exposed to seasonal variations mainly due to the meteorological conditions. The bottom water remains almost the same during the different seasons of the year.

To establish the circulation patterns in the southeastern sector of the Mediterranean Sea, oceanographic data must include current measurements. This will throw more light on the validity of the application of the circulation theorem involving the relationship between the field of seawater density and the current velocity field.

SUMMARY

The dynamic topography of the southeastern sector of the Mediterranean Sea is shown during the flood season before the High Dam and during the winter season for three depths, surface, 50 m, and 100 m. The principle of Defant (1941) for reference level was applied at offshore stations, while the method of Groen (1948) was used at coastal stations. One hundred and fifty hydrographic stations were used in the analysis. The level of no motion is between the 200 to 300 m layer for the offshore stations. The T-S diagrams show the interaction between atmosphere and sea on the water masses during the winter season, and the effect of the Nile flood before and after the construction of the High Dam. Comparisons between observed and calculated-geostrophic current during the summer confirms that the geostrophic circulation constitutes the principal components of the total circulation. The circulation pattern for late summer (October) is noticeably distinguishable from that for the winter season.

REFERENCES

- Defant, A. 1941. Physical oceanography. Vol. I. Pergamon Press, New York.
- Emery, K. O. and C. J. George. 1963. The shores of Lebanon. Woods Hole Oceanogr. Inst., No. 1385.
- Engel, I. 1967. Currents in the Eastern Mediterranean. *Internat. Hydrogr. Rev.*, 44 (2), pp. 23—40.
- Gorgy, S. 1966. Les pêcheries et le milieu marin dans le secteur méditerranéen de la République Arabe Unie. Thèses Doctorat, Université Paris.
- Groen, P. 1948. Methods for estimating dynamic slopes and currents in shallow water. *J. Mar. Res.*, 7 (3), pp. 313—316.
- Guibout, P. 1972. Project Eastern Mediterranean 1967—68. Rapport Technique OTAN No. 60.

- Lacombe, H. and P. Tchernia. 1960. Quelques traits généraux de l'hydrologie Méditerranéenne, dans le proche Atlantique et dans le détroit de Gibraltar. *Cahier Océanogr.*, 12 (8), pp. 527—547.
- Ovtchinnikov, I. M. 1966. Circulation in the surface and intermediate layers of the Mediterranean. (in Russian) *Okeanologija*, 6 (1), pp. 62—75.
- Pollak, M. J. 1951. The sources of the deep water of the Eastern Mediterranean Sea. *J. Mar. Res.*, 10 (1), pp. 128—152.
- Sharaf El Din, S. H. 1972. Some aspects of the hydrographic conditions of the Eastern part of the Mediterranean Sea. *Rapp. Comm. int. Mer. Médit.*, 20 (4), pp. 619—621.
- Sharaf El Din, S. H. 1972. Longshore sand transport in the surface zone along the Egyptian coast. *Second Internat. Ocean Develop. Conf. Exhib.*, Tokyo, Japan.
- Wüst, G. 1961. On the vertical circulation of the Mediterranean Sea. *J. Geophys. Res.*, 66 (10), p. 3261.

GEOSTROFIČKE STRUJE U JUGOISTOČNOM DIJELU MEDITERANA

Sayed H. Sharaf El Din

Odjel za oceanografiju, Sveučilište u Aleksandriji, Aleksandrija, Egipat

i

Amin M. Karam

Institut za oceanografiju i ribarstvo, Aleksandrija, Egipat

KRATAK SADRŽAJ

Prikazana je dinamička topografija jugoistočnog sektora Mediterana u sezoni poplava prije izgradnje brane na Nilu i za zimu na tri dubine: površini, 50 i 100 m. Referentna dubina za vanjske postaje je određena prema Defantu (1941), a za obalne postaje prema Groenu (1948). Upotrebljeni su podaci sa 150 postaja. Dubina mirovanja je za vanjske postaje u sloju od 200—300 m. T—S dijagrami pokazuju djelovanje atmosfere na vodene mase u zimskoj sezoni kao i utjecaj dotoka Nila prije i poslije izgradnje velike brane. Usporedba motrenih i izračunatih struja za ljetu pokazuje da geostrofička cirkulacija predstavlja glavnu komponentu strujanja. Strujanje u kasnom ljetu (listopad) se jako razlikuje od zimskog strujanja.

